A Journal of the Gesellschaft Deutscher Chemiker

Angewandte International Edition GDCh Chemie

www.angewandte.org

## Accepted Article

**Title:** Substrate Induced Dimerization Assembly of Chiral Macrocycle Catalysts toward Cooperative Asymmetric Catalysis

**Authors:** Hao Guo, Lie-Wei Zhang, Hao Zhou, Wei Meng, Yu-Fei Ao, De-Xian Wang, and Qi-Qiang Wang



**To be cited as:** *Angew. Chem. Int. Ed.* 10.1002/anie.201910399
*Angew. Chem.* 10.1002/ange.201910399

**Link to VoR:** http://dx.doi.org/10.1002/anie.201910399
http://dx.doi.org/10.1002/ange.201910399

WILEY-VCH

10.1002/anie.201910399


WILEY-VCH

# Substrate Induced Dimerization Assembly of Chiral Macrocycle Catalysts toward Cooperative Asymmetric Catalysis

Hao Guo,[a,b] Lie-Wei Zhang,[a,b] Hao Zhou,[a,b] Wei Meng,[a] Yu-Fei Ao,[a] De-Xian Wang,[a,b] and Qi-Qiang Wang*[a,b]

**Abstract:** We reported herein a rare artificial system on substrate-induced dimerization assembly of chiral macrocycle catalysts, enabling a highly cooperative hydrogen-bonding activation network for efficient and enantioselective transformation. These macrocycles contain two thiourea and two chiral diamine moieties and were found to dimerize with sulfate to form a sandwich-like assembly. Upon dimerization, the macrocycles adopt an extended conformation and reciprocally complement the hydrogen-bonding interaction sites. Inspired by the guest-induced dynamic assembly, these macrocycles were applied on catalyzing decarboxylative Mannich reaction of cyclic aldimines containing a sulfamate heading group. As anticipated, the imine substrate can be activated toward nucleophilic attack of *β*-ketoacid through a highly cooperative hydrogen-bonding network enabled by sulfamate-induced dimerization assembly of the macrocycle catalysts. By this strategy, highly efficient (>95% yield in most cases) and enantioselective (up to 97.5:2.5 er) transformation of a variety of substrates using only 5 mol% macrocycle was achieved, providing a potent means for organocatalytic asymmetric transformation of the titled reactions.

Taking the inspiration of enzyme catalysis, many cavity-containing macrocycle and cage compounds have been applied as supramolecular catalysts to facilitate otherwise disfavored transformation.[1-4] One important feature of enzyme catalysis is induced-fit of substrate and active sites to obtain most favorable interactions for maximum transition state stabilization.[5-6] This induced-fit can sometimes operate through cooperation of individual proteins by reciprocal complementation of their active sites.[5] For example, dynamin, a prototypical member of GTPases, has been recently shown to undergo G domain dimerization that leads to assembly-stimulated catalytic activity.[7] For synthetic catalytic systems, however, the substrate-induced catalyst assembly and regulatory mechanism are underdeveloped. Among the only few examples, Otto et al. nicely showed transient, substrate-induced macrocyclic catalyst formation in a disulfide-based dynamic combinatorial library.[8] Prins and Chen et al. demonstrated that a phosphate ester substrate can induce the formation of vesicular assemblies which act as cooperative catalysts for hydrolysis of the same substrate.[9] A substrate induced covalent assembly formation of chiral boroxinate catalysts has also been shown by Wulff et al. on catalyzing asymmetric cycloaddition reactions.[10] Herein we reported the first example of substrate-induced noncovalent dimerization assembly of chiral macrocycle catalysts, which enables a highly cooperative hydrogen-bonding network for efficient and enantioselective transformation.

Recently we initiated a project on construction of macrocycle catalysts by taking prominent catalytic groups as direct building components to form macrocyclic scaffolds. In this way, the definitive catalytic functionalities can be integrated and eternally embedded within a confined macrocyclic cavity. We chose thiourea, specially diarylthiourea units, as the building components due to their superior binding and activation abilities.[11-15] A series of chiral diamine scaffolds were incorporated as linkers to, on one hand, introduce a chiral environment, and on other hand, furnish bifunctional thiourea-Lewis base sites for dual activation of both electrophile and nucleophile.[16] Following this design, the multifunctionalized tetraamino-bisthiourea chiral macrocycles **M1**-**M4** were constructed (Scheme 1). In **M3** and **M4**, the hetero-combination of different diamine linkers as well as the diastereomeric forms was intended to provide a delicate control on both macrocyclic conformation and chiral microenvironment.

The synthesis of the chiral macrocycles was straightforward and gram-scale preparation can be easily realized (see Supporting Information). Enantiomerically pure dimethylated 1,2-cyclohexanediamine or 1,2-diphenylethylenediamine was firstly reacted with two equiv. 3-nitro-5-trifluoromethylbenzyl bromide, followed by nitro reduction, affording bis-amine fragments which can be further converted to bis-isothiocyanates in high yields. Macrocyclization between bis-amine and bis-isothiocyanate fragments went smoothly and gave the final chiral macrocycles in 39%-72% yields.

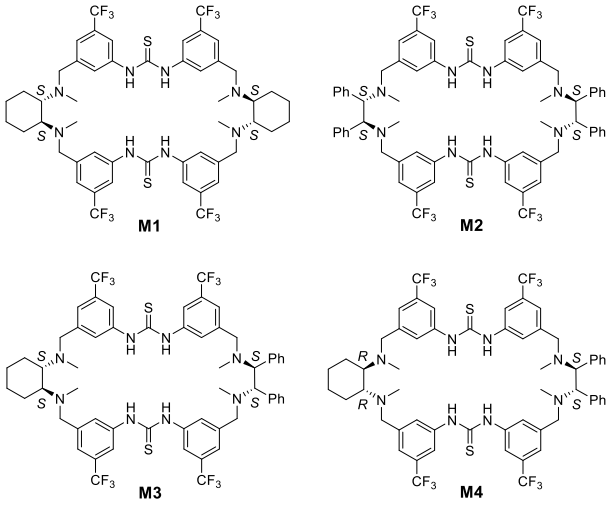


**Scheme 1.** Structure of the tetraamino-bisthiourea chiral macrocycles.

[a] Mr. H. Guo, Ms. L.-W. Zhang, Mr. H. Zhou, Dr. W. Meng, Dr. Y.-F. Ao, Prof. Dr. D.-X. Wang, Prof. Dr. Q.-Q. Wang
Beijing National Laboratory for Molecular Sciences, CAS Key Laboratory of Molecular Recognition and Function
Institute of Chemistry, Chinese Academy of Sciences
Beijing 100190, China
E-mail: qiqiangw@iccas.ac.cn
[b] Mr. H. Guo, Ms. L.-W. Zhang, Mr. H. Zhou, Prof. Dr. D.-X. Wang, Prof. Dr. Q.-Q. Wang
University of Chinese Academy of Sciences
Beijing 100049, China

Supporting information for this article is given via a link at the end of the document.

During binding studies of these macrocycles prior to catalysis, a complex crystal, $[(\mathbf{M1})_2{\bullet}SO_4^{2-}][TBA^+]_2$, was reproducibly obtained from a solution of **M1** and tetra(*n*-butyl)ammonium sulfate in acetonitrile. Crystal structure showed two macrocycles and one sulfate anion form a sandwich-like complex (Figure 1). Sulfate is embedded in between the two macrocycles, forming four pairs of bifurcated hydrogen bonds with the four thiourea groups from both macrocycles (N-H···O distances: 2.87-2.93 Å). The two macrocycles are packed crosswise so that the four thioureas are allowed to spatially surround the sulfate. In this packing way, the $CF_3$-attached benzene rings can enjoy π-π stacking with neighboring ones and also avoid steric hindrance between the bulky $CF_3$ groups. Upon dimerization, the macrocycle adopts an extended conformation and forms an exposing cleft. This is in contrast to a self-folded conformation in the monomeric chloride complex $[\mathbf{M1}{\bullet}(Cl^-)_2][TBA^+]_2$ where two aryl-thiourea moieties are packed onto each other (Figure S1).

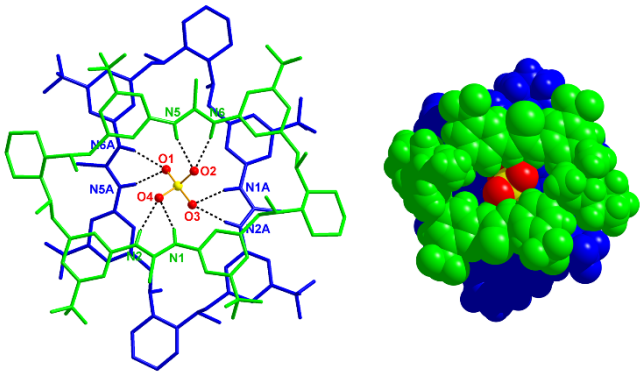


**Figure 1.** Crystal structure of $[(\mathbf{M1})_2{\bullet}SO_4^{2-}][TBA^+]_2$. $TBA^+$ counterions are omitted for clarity. H-bonding distances: N1-H···O4, 2.917; N2-H···O4, 2.929; N5-H···O2, 2.917; N6-H···O2, 2.899; N1A-H···O3, 2.898; N2A-H···O3, 2.901; N5A-H···O1, 2.867; N6A-H···O1, 2.902 Å.

The sulfate-induced macrocycle dimerization was also observed in solution. As shown by $^1$H NMR titrations, upon addition of sulfate to the solution of **M1**, a new set of signals, including significantly downfield shifted N*H* signal (Δδ = 3.0 ppm), gradually emerged and became dominant at about 0.5 eq. of sulfate (Figure S2). At this point, the original macrocycle signals almost completely disappeared. This was consistent with 2:1 macrocycle-sulfate assembly formation. The slow-exchange dynamic and the dominant assembly signals suggested a strong dimerization tendency. With excess of sulfate, a second set of signals started to appear, which can be assigned to 1:1 macrocycle-sulfate complex. The strong dimerization tendency was also suggested by high-resolution ESI-MS, where predominant peaks corresponding to $[(\mathbf{M1})_2{\bullet}SO_4^{2-}]$ and related species were observed (Figure S6). For **M2**-**M4**, similar dimerization assembly was also observed (Figures S2-S9).

Upon sulfate-induced dimerization, the macrocycles adopt an extroversive conformation and reciprocally complement the interaction sites. As inspired by the induced-fit regulation of enzymes, we wondered if this dynamic assembly system can be applied on cooperative catalysis. Decarboxylative Mannich reaction of cyclic aldimines **1** with *β*-ketoacids provides an alternative means to the direct Mannich reaction[17] for accessing valuable *β*-amino ketones, but efficient organocatalytic asymmetric transformation is lacking.[18] We speculated that the imine substrate could be activated toward nucleophilic attack through induced dimerization assembly of the chiral macrocycle catalysts (Figure 2). The generating negative charge on the sulfamate heading group (analogue to sulfate) could be stabilized through a cooperative H-bonding network enabled by the as-formed dimeric assembly. According to the modelling, the exposing cleft on the assembly surface is suitable for incoming ketoacid substrate that is activated through deprotonation by the tertiary amine site (Figure S33).

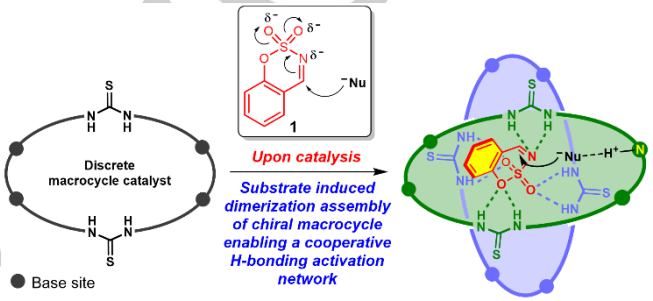


**Figure 2.** Proposed mode for substrate-induced dimerization assembly of chiral macrocycle catalysts toward cooperative asymmetric catalysis.

The reaction between **1a** and **2a** was initially performed in 1,4-dioxane with a 2 mol% loading of the chiral macrocycles (Table S2). The reaction went very quickly and achieved complete conversion in 20 min. While **M1**-**M3** gave a low enantiomeric ratio (er), **M4** enabled a considerable enantioselectivity (74:26 er). This suggests subtle structural change on the macrocycle could have a large influence on asymmetric induction. Solvent screening showed THF was the best (Table S2). Increasing the macrocycle loading to 5 mol% led to a further improved enantioselectivity (85:15 er) and complete conversion in 5 min, suggesting a very high efficiency (Table 1, entry 4). Decreasing reaction temperature to 0 °C resulted in a better selectivity (Table 1, entry 7). Finally, the reaction concentration was also screened. Under optimal conditions (5 mol% **M4**, THF, *c* 0.05 M, -10 °C), 99% yield and a high enantioselectivity (94:6 er) was achieved (Table 1, entry 12). As anticipated, in the presence of only 2.5 mol% $(TBA^+)_2SO_4^{2-}$, the enantioselectivity was totally lost, implying that sulfate can replace the imine substrate by occupation within the assembly (Table 1, entry 14).

To gain more insight on the catalytic mechanism, a series of experiments were performed. 2:1 binding species between the macrocycle and imine substrate can be detected by ESI-MS with a signal of $[2\mathbf{M4} + \mathbf{1a}]^-$ observed (Figure S12). The in situ ESI-MS analysis of the reaction mixture was also carried out (Figure 3a and Figure S20). Multiple signals corresponding to the addition intermediate $\mathbf{A}^-$ and its macrocycle-associated species were observed, indicating that the reaction operates by the Mannich addition of the *β*-ketoacid to the imine prior to subsequent decarboxylation.[19] Especially, in the very high m/z

10.1002/anie.201910399



WILEY-VCH

**Table 1.** Reaction optimization for macrocycle-catalyzed decarboxylative Mannich reaction of cyclic aldimine **1a** with *β*-ketoacid **2a**.[a]

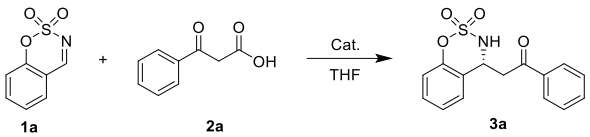


| Entry | Cat. (mol%) | *T* [°C] | Conc. [M][d] | Time | Yield [%][e] | er[f] |
|---|---|---|---|---|---|---|
| 1 | **M4** (2%) | 25 | 0.2 | 20 min | 99 | 81.5:18.5 |
| 2 | **M4** (0.5%) | 25 | 0.2 | 60 min | 99 | 81:19 |
| 3 | **M4** (1%) | 25 | 0.2 | 40 min | 98 | 81.5:18.5 |
| 4 | **M4** (5%) | 25 | 0.2 | 5 min | 99 | 85:15 |
| 5 | **M4** (10%) | 25 | 0.2 | 5 min | 99 | 85.5:14.5 |
| 6[b] | **M4** (5%) | 25 | 0.2 | 10 min | 98 | 85.5:14.5 |
| 7[b] | **M4** (5%) | 0 | 0.2 | 90 min | 99 | 89.5:10.5 |
| 8[b] | **M4** (5%) | -20 | 0.2 | 8 h | 99 | 85.5:14.5 |
| 9[b] | **M4** (5%) | 0 | 0.1 | 100 min | 99 | 92:8 |
| 10[b] | **M4** (5%) | 0 | 0.05 | 100 min | 98 | 93:7 |
| 11[b] | **M4** (5%) | 0 | 0.033 | 2 h | 99 | 91.5:8.5 |
| **12[b]** | **M4 (5%)** | **-10** | **0.05** | **3 h** | **99** | **94:6** |
| 13[b] | **M4** (5%) | -20 | 0.05 | 9 h | 98 | 94:6 |
| 14[b,c] | **M4** (5%) | -10 | 0.05 | 3 h | 99 | 51:49 |
| 15[b] | **M1** (5%) | -10 | 0.05 | 3.5 h | 99 | 51:49 |
| 16[b] | **M2** (5%) | -10 | 0.05 | 24 h | 99 | 62.5:37.5 |
| 17[b] | **M3** (5%) | -10 | 0.05 | 8 h | 99 | 63:37 |

[a] Reaction conditions: **1a** (0.2 mmol) and **2a** (1.5 equiv). [b] 1.2 equiv **2a** used. [c] In the presence of 2.5 mol% $(TBA^+)_2SO_4^{2-}$. [d] Concentration of **1a**. [e] Isolated yields after column chromatography. [f] Determined by HPLC analysis on a chiral stationary phase.

region, the signal of the dimeric species [2**M4** + **A**$^-$] can also be detected, implying that two macrocycles can work together to cooperatively bind and activate the substrates. During DFT optimization of macrocycle-complexed reaction species, a structure of the addition species captured within the dimeric assembly can be identified, showing the anticipated cooperative H-bonding network (Figure 3e).

Reaction kinetics analysis was performed and a second order dependence of the initial reaction rate on the concentration of **M4** was found, in line with the dimeric assembly catalysis mode (Figures 3b and 3c, and Figures S26-S32). Moreover, the relationship between the enantioselectivity of the reaction and the enantiomeric purity of **M4** was examined, and a slight positive non-linear effect was observed (Figure 3d). The small non-linear effect could reflect that the hetero-dimerization (**M4**, ***ent*-M4**) may not dominate as the homo-dimerization (**M4**, **M4**), or that their activity cannot be largely differentiated. Binding studies between ***rac*-M4** and sulfate showed the hetero-dimerization did co-exist with homo-dimerization (Figure S22). Interestingly, sulfate-induced dimerization between two different kinds of macrocycles (*e.g.* **M1**, **M4**) was also observed (Figures S23-S25). With this in mind, the catalyzed reactions using the two mixed macrocycle catalysts were also tested (Scheme 2A). While **M1** gave a very low but slightly positive ee (+2%), the 1:1 mixture of **M4**+**M1** gave 55% ee; however, an even higher ee (58%) was obtained for **M4**+***ent*-M1** (1:1). This opposite direction of the ee difference wouldn't be expected if the two kinds of macrocycle catalysts had operated independently, thus suggested a cooperative interaction of the two macrocycles.

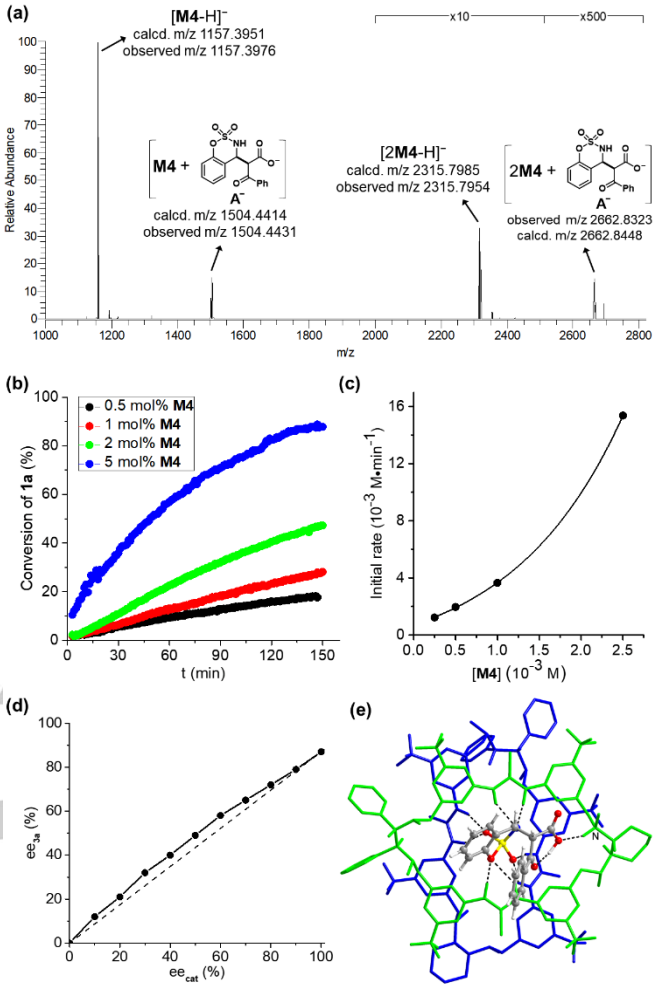


**Figure 3.** (a) HR ESI-MS of reaction mixture of **1a** and **2a** catalyzed by **M4**. (b) Conversion of **1a** over time and (c) the dependence of the initial reaction rate on concentration of **M4**. (d) Dependence of ee of the product **3a** on ee of **M4**. (e) DFT modelling (B3LYP/3-21G) of the addition intermediate fitting within the dimeric assembly. Nonessential hydrogen atoms are omitted for clarity.

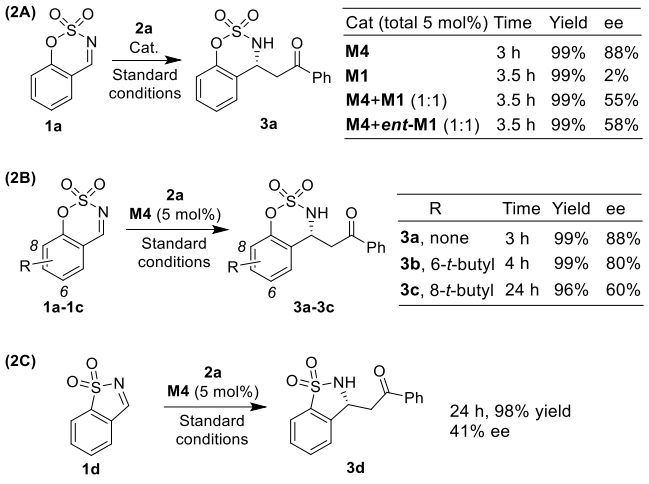


| Cat (total 5 mol%) | Time | Yield | ee |
|---|---|---|---|
| **M4** | 3 h | 99% | 88% |
| **M1** | 3.5 h | 99% | 2% |
| **M4**+**M1** (1:1) | 3.5 h | 99% | 55% |
| **M4**+***ent*-M1** (1:1) | 3.5 h | 99% | 58% |

| R | Time | Yield | ee |
|---|---|---|---|
| **3a**, none | 3 h | 99% | 88% |
| **3b**, 6-*t*-butyl | 4 h | 99% | 80% |
| **3c**, 8-*t*-butyl | 24 h | 96% | 60% |

**Scheme 2.** Comparison and control reactions. Conditions: **1** (0.2 mmol), **2a** (1.2 equiv), and macrocycle catalyst (5 mol%) in 4 mL of THF at -10 °C.

As the dimeric motif has a deep binding and activation pocket, imine substrates with different steric hinderance (**1a-1c**) were subjected (Scheme 2B). While the uncatalyzed reactions of the three substrates showed very similar reactivity, the catalyzed reaction of substrate **1c** with bulky *t*-butyl group adjacent to the sulfamate group was much slower and gave decreased ee compared to that of **1a** and **1b**. This suggests increased steric hinderance may interfere with the sulfamate heading group inserting within the assembly. For the 5-membered cyclic imine substrate **1d**, the reaction was also interfered (Scheme 2C), which could be due to that the sulfonamide heading group (analogue to sulfonate) cannot induce dimeric assembly formation (Figure S11).

Finally, substrate scope of the reaction was explored (Scheme 3). Regardless of the electron-donating and electron-withdrawing substituents on both the cyclic aldimines (6-position) and phenyl *β*-ketoacids, high yield (>95% in most cases) and enantioselectivity (up to 97.5:2.5 er) was achieved. As noticed, the substitution changed to *7* and *8*-position of the cyclic aldimine slowed down the reaction (*e.g.* **3e** *vs* **3f** *vs* **3g**, **3o** vs **3p**) and even disrupted the enantioselectivity (**3p**). This reflects the steric effect when the sulfamate heading group inserting within the assembly.

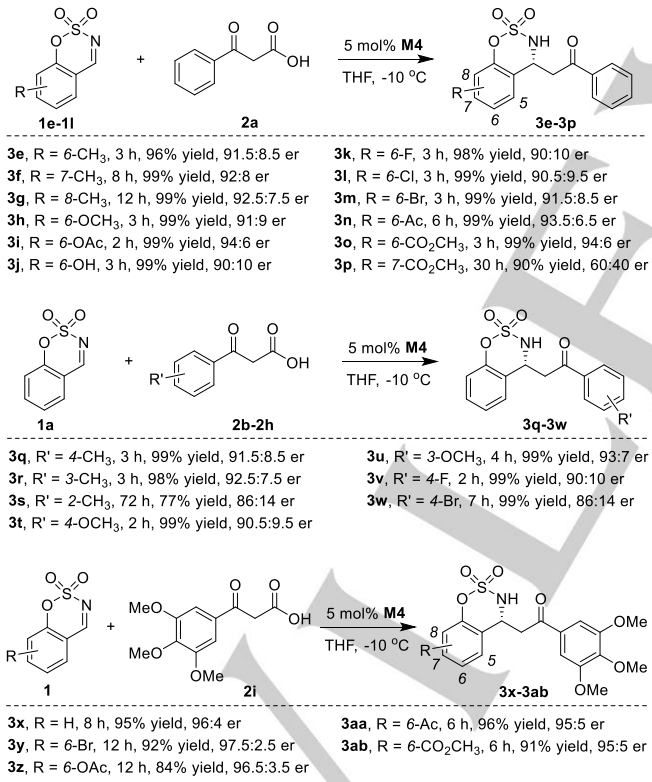


**Scheme 3.** Substrate scope. Reaction conditions: **1** (0.2 mmol), **2** (1.2 equiv), and **M4** (5 mol%) in 4 mL of THF at -10 °C.

In conclusion, a series of multifunctionalized tetraamino-bisthiourea chiral macrocycles were synthesized. These chiral macrocycles tend to dimerize with sulfate to form a sandwich-like assembly. Through dimerization, an extended macrocyclic conformation and a reciprocal complementation of the interaction sites was achieved. Taking these advantages, this dynamic assembly system was applied on catalyzing decarboxylative Mannich reaction of cyclic aldimine substrates containing a sulfamate heading group. The sulfamate-induced dimerization of the chiral macrocycles provided a highly cooperative hydrogen-bonding network for activating the imine substrate itself toward the nucleophilic attack of *β*-ketoacid. This system enabled highly efficient and enantioselective transformation of a variety of substrates, providing a potent means for organocatalytic asymmetric transformation of the titled reactions. This substrate-induced chiral catalyst assembly, resembling induced-fit regulation of an enzyme, complements the conventional asymmetric catalytic principles and would enrich the exploitation of efficient artificial catalysis systems toward challenging transformations.

## Acknowledgements

Financial supports from National Natural Science Foundation of China (21871276, 21502200, 21521002) and Chinese Academy of Sciences (QYZDJ-SSW-SLH023) are gratefully acknowledged.

**Keywords:** supramolecular catalysis • chiral macrocycles • self-assembly • anion binding • cooperative asymmetric catalysis

[1] a) P. W. N. M. van Leeuwen, *Supramolecular Catalysis*, Wiley-VCH, Weinheim, **2008**; b) M. Raynal, P. Ballester, A. Vidal-Ferran, P. W. N. M. van Leeuwen, *Chem. Soc. Rev.* **2014**, *43*, 1734-1787; c) S. H. A. M. Leenders, R. Gramage-Doria, B. de Bruin, J. N. H. Reek, *Chem. Soc. Rev.* **2015**, *44*, 433-448.

[2] a) R. Breslow, S. D. Dong, *Chem. Rev.* **1998**, *98*, 1997-2011; b) R. J. Hooley, J. Rebek, Jr. *Chem. Bio.* **2009**, *16*, 255-264; c) K. I. Assaf, W. M. Nau, *Chem. Soc. Rev.* **2015**, *44*, 394-418; d) N. Le Poul, Y. Le Mest, I. Jabin, O. Reinaud, *Acc. Chem. Res.* **2015**, *48*, 2097-2106; e) D. Zhang, A. Martinez, J. Dutasta, *Chem. Rev.* **2017**, *117*, 4900-4942; f) Y. Yu, J. Rebek, Jr. *Acc. Chem. Res.* **2018**, *51*, 3031-3040.

[3] Q.-Q. Wang, *Supramolecular Catalysis Using Organic Macrocycles*, Chapter in Handbook of Macrocyclic Supramolecular Assembly, Y. Liu, Y. Chen, H.-Y. Zhang, Eds. Springer, Singapore, **2019**.

[4] a) T. S. Koblenz, J. Wassenaar, J. N. H. Reek, *Chem. Soc. Rev.* **2008**, *37*, 247-262; b) M. Yoshizawa, J. K. Klosterman, M. Fujita, *Angew. Chem.* **2009**, *121*, 3470-3490; *Angew. Chem. Int. Ed.* **2009**, *48*, 3418-3438; c) C. J. Brown, F. D. Toste, R. G. Bergman, K. N. Raymond, *Chem. Rev.* **2015**, *115*, 3012-3035; d) Q. Zhang, L. Catti, K. Tiefenbacher, *Acc. Chem. Res.* **2018**, *51*, 2107-2114; e) C. Tan, D. Chu, X. Tang, Y. Liu, W. Xuan, Y. Cui, *Chem. Eur. J.* **2019**, *25*, 662-672.

[5] a) J. P. Changeux, S. J. Edelstein, *Science* **2005**, *308*, 1424-1428; b) J. Kuriyan, D. Eisenberg, *Nature* **2007**, *450*, 983-990.

[6] M. Juríček, N. L. Strutt, J. C. Barnes, A. M. Butterfield, E. J. Dale, K. K. Baldridge, J. F. Stoddart, J. S. Siegel, *Nature Chem.* **2014**, *6*, 222-228.

[7] a) R. Gasper, S. Meyer, K. Gotthardt, M. Sirajuddin, A. Wittinghofer, *Nature Rev. Mol. Cell Biol.* **2009**, *10*, 423-429; b) J. S. Chappie, S. Acharya, M. Leonard, S. L. Schmid, F. Dyda, *Nature* **2010**, *465*, 435-441.

[8] a) B. Brisig, J. K. M. Sanders, S. Otto, *Angew. Chem.* **2003**, *115*, 1308-1311; *Angew. Chem. Int. Ed.* **2003**, *42*, 1270-1273; b) H. Fanlo-Virgós, A.-N. R. Alba, S. Hamieh, M. Colomb-Delsuc, S. Otto, *Angew. Chem.*

**2014**, *126*, 11528-11532; *Angew. Chem. Int. Ed.* **2014**, *53*, 11346-11350.

[9] P. S. Muñana, G. Ragazzon, J. Dupont, C. Z.-J. Ren, L. J. Prins, J. L.-Y. Chen, *Angew. Chem.* **2018**, *130*, 16707-16712; *Angew. Chem. Int. Ed.* **2018**, *57*, 16469-16474.

[10] G. Hu, A. K. Gupta, R. H. Huang, M. Mukherjee, W. D. Wulff, *J. Am. Chem. Soc.* **2010**, *132*, 14669-14675.

[11] a) A.-F. Li, J.-H. Wang, F. Wang, Y.-B. Jiang, *Chem. Soc. Rev.* **2010**, *39*, 3729-3745; b) V. Amendola, L. Fabbrizzi, L. Mosca, *Chem. Soc. Rev.* **2010**, *39*, 3889-3915.

[12] a) P. R. Schreiner, *Chem. Soc. Rev.* **2003**, *32*, 289-296; b) Z. Zhang, P. R. Schreiner, *Chem. Soc. Rev.* **2009**, *38*, 1187-1198.

[13] L. S. Shimizu, S. R. Salpage, A. A. Korous, *Acc. Chem. Res.* **2014**, *47*, 2116-2127.

[14] Y. Park, K. C. Harper, N. Kuhl, E. E. Kwan, R. Y. Liu, E. N. Jacobsen, *Science* **2017**, 355, 162-166.

[15] R. Ning, Y.-F. Ao, D.-X. Wang, Q.-Q. Wang, *Chem. Eur. J.* **2018**, *24*, 4268-4272.

[16] a) Y. Takemoto, *Org. Biomol. Chem.* **2005**, *3*, 4299-4306; b) S. J. Connon, *Chem. Commun.* **2008**, 2499-2510; c) X. Fang, C.-J. Wang, *Chem. Commun.* **2015**, *51*, 1185-1197.

[17] a) Y.-Q. Wang, X.-Y. Cui, Y.-Y. Ren, Y. Zhang, *Org. Biomol. Chem.* **2014**, *12*, 9101-9104; b) X.-Y. Cui, H.-X. Duan, Y. Zhang, Y.-Q. Wang, *Chem. Asian J.* **2016**, *11*, 3118-3125.

[18] a) H.-X. Zhang, J. Nie, H. Cai, J.-A. Ma, *Org. Lett.* **2014**, *16*, 2542-2545; b) B.-N. Lai, J.-F. Qiu, H.-X. Zhang, J. Nie, J.-A. Ma, *Org. Lett.* **2016**, *18*, 520-523; c) Y.-J. Liu, J.-S. Li, J. Nie, J.-A. Ma, *Org. Lett.* **2018**, *20*, 3643-3646.

[19] H.-N. Yuan, S. Wang, J. Nie, W. Meng, Q. Yao, J.-A. Ma, *Angew. Chem.* **2013**, *125*, 3961-3965; *Angew. Chem. Int. Ed.* **2013**, *52*, 3869-3873.

10.1002/anie.201910399


WILEY-VCH

**Entry for the Table of Contents**

# COMMUNICATION

**It takes two to tango:** a rare example on substrate-induced dimerization assembly of chiral macrocycle catalysts, which enables a highly cooperative hydrogen-bonding activation network for efficient and enantioselective transformation, was realized.

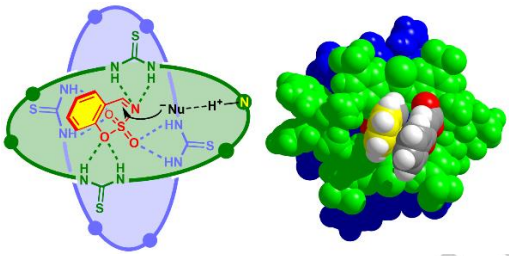

*Hao Guo, Lie-Wei Zhang, Hao Zhou, Wei Meng, Yu-Fei Ao, De-Xian Wang, and Qi-Qiang Wang**

***Page No. – Page No.***

**Substrate Induced Dimerization Assembly of Chiral Macrocycle Catalysts toward Cooperative Asymmetric Catalysis**